ELSEVIER

Biochimica et Biophysica Acta 1418 (1999) 335–343

BIOCHIMICA ET BIOPHYSICA ACTA
BBA

An X-ray diffraction study of the effect of α-tocopherol on the structure and phase behaviour of bilayers of dimyristoylphosphatidylethanolamine

Xiaoyuan Wang [a], Hiroshi Takahashi [b], Ichiro Hatta [b], Peter J. Quinn [a,*]

[a] *Division of Life Sciences, King's College London, Campden Hill, London W8 7AH, UK*
[b] *Department of Applied Physics, Nagoya University, Nagoya 464-8603, Japan*

Received 29 October 1998; received in revised form 15 February 1999; accepted 9 March 1999

Abstract

The effect of α-tocopherol on the thermotropic phase transition behaviour of aqueous dispersions of dimyristoylphosphatidylethanolamine was examined using synchrotron X-ray diffraction methods. The temperature of gel to liquid-crystalline ($L_\beta \rightarrow L_\alpha$) phase transition decreases from 49.5 to 44.5°C and temperature range where gel and liquid-crystalline phases coexist increases from 4 to 8°C with increasing concentration of α-tocopherol up to 20 mol%. Codispersion of dimyristoylphosphatidylethanolamine containing 2.5 mol% α-tocopherol gives similar lamellar diffraction patterns as those of the pure phospholipid both in heating and cooling scans. With 5 mol% α-tocopherol in the phospholipid, however, an inverted hexagonal phase is induced which coexists with the lamellar gel phase at temperatures just before transition to liquid-crystalline lamellar phase. The presence of 10 mol% α-tocopherol shows a more pronounced inverted hexagonal phase in the lamellar gel phase but, in addition, another non-lamellar phase appears with the lamellar liquid-crystalline phase at higher temperature. This non-lamellar phase coexists with the lamellar liquid-crystalline phase of the pure phospholipid and can be indexed by six diffraction orders to a cubic phase of Pn3m or Pn3 space groups and with a lattice constant of 12.52 ± 0.01 nm at 84°C. In mixed aqueous dispersions containing 20 mol% α-tocopherol, only inverted hexagonal phase and lamellar phase were observed. The only change seen in the wide-angle scattering region was a transition from sharp symmetrical diffraction peak at 0.43 nm, typical of gel phases, to broad peaks centred at 0.47 nm signifying disordered hydrocarbon chains in all the mixtures examined. Electron density calculations through the lamellar repeat of the gel phase using six orders of reflection indicated no difference in bilayer thickness due to the presence of 10 mol% α-tocopherol. The results were interpreted to indicate that α-tocopherol is not randomly distributed throughout the phospholipid molecules oriented in bilayer configuration, but it exists either as domains coexisting with gel phase bilayers of pure phospholipid at temperatures lower than T_m or, at higher temperatures, as inverted hexagonal phase consisting of a defined stoichiometry of phospholipid and α-tocopherol molecules.

Keywords: α-Tocopherol; Phosphatidylethanolamine; Vitamin E; X-ray diffraction

1. Introduction

Vitamin E (α-tocopherol) is an ubiquitous lipid component of biological membranes. Its function in biological membranes is believed to act as an antioxidant to prevent oxidation of unsaturated membrane lipids [1–4] and in addition to serve as a membrane stabiliser [5]. In order to understand the biological functions of α-tocopherol at the molecular level, it is

* Corresponding author. Fax: +44 (171) 333-4408; E-mail: p.quinn@kcl.ac.uk

0005-2736/99/$ – see front matter
PII: S0005-2736(99)00044-9

essential to understand the interaction between α-tocopherol and phospholipids that represent the major components of the membrane lipid bilayer matrix. The effect of α-tocopherol on the phase behaviour of model phospholipid bilayer membranes has, therefore, been widely studied using a variety of biophysical techniques. These studies have revealed that the effect of α-tocopherol on phosphatidylcholines is similar in many respects to that of cholesterol, i.e. addition of α-tocopherol increases the temperature range and reduces the enthalpy of $L_\beta \rightarrow L_\alpha$ phase transition of phosphatidylcholines [6–10]. Moreover, α-tocopherol causes an increase in the order parameter and a decrease in fluidity of the hydrocarbon domain of the bilayer [11–13]. The proportion of α-tocopherol in most biological membranes rarely exceeds 2 mol% with respect to the total membrane lipid, but α-tocopherol may be concentrated in some domain where its proportion could be much higher. The structural effects of α-tocopherol, as revealed by X-ray diffraction studies, have been interpreted as the formation of phosphatidylcholine/α-tocopherol complexes with an approximate stoichiometry of 10:1. The complexes exist in both gel and fluid phases of the phospholipid [10].

Taking into account the heterogeneous phospholipid composition of biological membranes, studies of the effect of α-tocopherol on phospholipid classes other than phosphatidylcholines, such as phosphatidylethanolamines, would also be instructive. Phosphatidylethanolamines are a class of phospholipids found abundantly in many biological membranes. Several studies have been reported of the effects of α-tocopherol on the $L_\beta \rightarrow L_\alpha$ phase transition of phosphatidylethanolamines [9,14,15]; these effects of α-tocopherol appear to differ only slightly from that of cholesterol on phosphatidylethanolamines [16–19]. Nevertheless, the amount of information on the structural effects of α-tocopherol on phosphatidylethanolamines is fairly limited and more detailed studies are required.

The present study was undertaken to examine the effect of α-tocopherol on the $L_\beta \rightarrow L_\alpha$ phase transition of dimyristoylphosphatidylethanolamine from the viewpoint of structural changes associated with the phase transition. We performed synchrotron X-ray diffraction studies of dimyristoylphosphatidylethanolamine/α-tocopherol mixtures to obtain real-time structural information during temperature scans through the $L_\beta \rightarrow L_\alpha$ phase transition. We present evidence that phase separations are created in the codispersions of the phospholipid with relatively high concentrations of α-tocopherol.

2. Materials and methods

To determine the effect of α-tocopherol on the phase behaviour of phosphatidylethanolamine bilayer dispersions, phospholipid was codispersed with 0, 2.5, 5, 10 or 20 mol% α-tocopherol and examined by real-time synchrotron X-ray diffraction measurements during heating and cooling scans. 1,2-Dimyristoyl-*sn*-phosphatidylethanolamine (DMPE) was purchased from Avanti Polar Lipids (Alabaster) and α-tocopherol from Acros Organics (Geel, Belgium). The lipids were dissolved in chloroform and mixed in appropriate proportions to achieve the desired molar fractions (mol% = 100% × mole α-tocopherol / (mole α-tocopherol+mole DMPE)). The solvent was evaporated under a stream of oxygen-free dry nitrogen and stored for 24 h under vacuum to remove remaining traces of solvent. The lipid mixtures were hydrated at 80°C for at least 1 h and dispersed by a rotamixer until homogeneous dispersions were obtained. The lipid dispersions were stored at 0–4°C for 24 h before examination. The method of preparation and storage gave reproducible phase behaviour when samples prepared at different times were examined by X-ray diffraction.

Synchrotron X-ray diffraction experiments were performed using a monochromatic (0.15405 nm) focused X-ray beam at station 8.2 of the Daresbury Synchrotron Radiation Laboratory, UK. The camera configuration allowed detection of small-angle and wide-angle X-ray scattering with a minimum of parallax error [20]. The beamline generates a flux of 4×10^{10} photons per second with a focal spot size of 0.3×3 mm^2 ($V \times H$) when the synchrotron radiation source is operating at a nominal 200 mA. The samples were mounted in a slot (1×5 mm) cut in a 1-mm-thick copper plate sandwiched between a pair of thin mica sheets. The sandwich was clamped to the silver block containing the temperature sensing and modulating elements of a cryomicroscope stage (Linkam Scientific Instruments, UK). Temperature

scans in heating and cooling modes were performed at 2°/min over a temperature range 30–90°C. X-ray scattering intensities at small angles ($2\theta = 0.14$–$3.53°$) were recorded using a multiwire quadrant detector. X-ray scattering intensities at wide angles ($2\theta = 8.6$–$45°$) were recorded using an INEL curved linear-wire detector (Instrumentation Electronique, France). Data were acquired in 400 consecutive time frames of 5 s and separated by a dead time between frames of 50 ms. Experimental data were analysed using the OTOKO software (EMBL, Hamburg, Germany) program [21]. Scattering intensities at small angles were corrected for fluctuations in beam intensity and detector response recorded from an ^{55}Fe source. Spatial calibrations were obtained using 21-orders of wet rat-tail collagen ($d = 67$ nm) [22]. The scattering intensity data recorded by the INEL detector was corrected for scattering from an empty cell and spatial calibrations were established from high-density polyethylene (0.4166, 0.3780 and 0.3014 nm) [23]. Samples were heated to 80°C prior to recording the first cooling scan to avoid unnecessary exposure of the sample to the X-ray beam. The reciprocal spacing $S = 1/d = 2\sin(\theta)/\lambda$, where d, λ, θ are the repeat distance, X-ray wave length and the diffraction angle, respectively.

Some static X-ray diffraction measurements were carried out using a Ni-filtered CuK_α radiation source (RU200BEH, Rigaku, Tokyo, Japan) and a two-dimensional area detector (Imaging plate, Fuji Photo Film, Tokyo, Japan). The X-ray beam was focused with a double-mirror optical system. The sample was sealed in a thin-wall quartz capillary of 1.0 mm diameter (Hilgenberg, Malsfeld, Germany). The capillary was cradled into a hollow brass holder. Temperature of the sample was controlled within ± 0.1°C by circulating water from a temperature-controlled water bath (B. Braun, Melsungen, Germany) through the sample mount.

To calculate electron density profiles, the observed intensities of the lamellar reflections were corrected for the Lorentz and polarisation factors, scaled, normalised and converted to structure amplitudes according to standard methods [24]. Phases of the reflections were determined from the analysis of plots of structure amplitudes as a function of the reciprocal space (S), using the Shannon sampling theorem [25–27]. The value of the structure amplitude at the zero of reciprocal space was estimated by the method proposed by King and Worthington [28]. To obtain a plot of structure amplitudes the thickness of the water layers between the bilayers of lipid was varied by application of an osmotic stress according to the method of McIntosh and Simon [29]. Liposome samples were prepared in aqueous solutions of polyvinylpyrrolidone of average molecular weight 40 000 (Sigma, Poole, UK).

3. Results

Plots of X-ray diffraction patterns recorded during a heating scan from 30 to 90°C at 2°C/min of pure DMPE are shown in Fig. 1. The scattering intensity patterns in the small-angle region (Fig. 1a) correspond to the first-order lamellar repeat spacing of the fully hydrated phospholipid and the wide-angle region (Fig. 1b) to the packing of the acyl chains of the phospholipid. It can be seen that the phospholipid undergoes a $L_\beta \rightarrow L_\alpha$ transition at 49.5°C. This

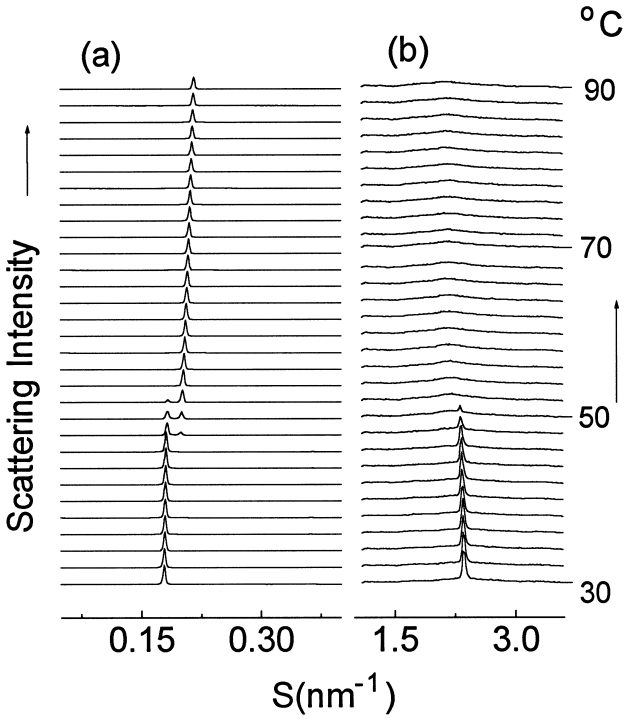

Fig. 1. Plots of successive X-ray scattering intensity profiles versus reciprocal spacing recorded during heating from 30 to 90°C at 2°/min of a fully hydrated dispersion of DMPE in the small-angle (a) and wide-angle (b) scattering regions. Each diffraction pattern represents scattering accumulated in 20 s.

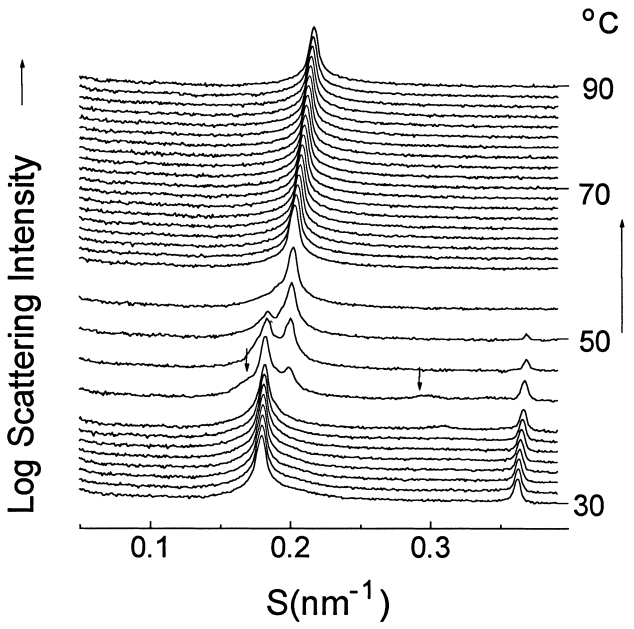

Fig. 2. Plots of successive X-ray scattering intensity profiles in the small-angle region versus reciprocal spacing recorded during heating from 30 to 90°C at 2°/min of a fully hydrated codispersion of 5 mol% α-tocopherol in DMPE. Each diffraction pattern represents scattering accumulated in 20 s. The profiles were plotted on a logarithmic scale to emphasise the minor bands. The arrows indicate diffraction peaks assigned to first- and second-order reflections of an inverted hexagonal phase.

is characterised by a change from sharp symmetrical diffraction peaks at 0.43 nm (48°C), typical of gel phases, to broad peaks centred at 0.46 nm in wide-angle region which coincides with a decrease of the lamellar repeat spacing from 5.5 nm (48°C) to 4.9 nm (52°C) seen in the small-angle scattering region. At temperatures in the region of the transition gel and fluid phases are seen to coexist indicating a two-state transition with no detectable intermediate phases. No transition to H_{II} phase was observed.

Codispersions of DMPE containing 2.5 mol% α-tocopherol (data not shown) gave similar small-angle patterns in heating and cooling scans as those presented in Fig. 1. 5 mol% α-tocopherol in the phospholipid induces appearance of another phase with spacings consistent with an inverted hexagonal phase coexisting with the lamellar gel phase at about 45°C. This can be seen in Fig. 2 which shows plots of X-ray diffraction patterns recorded during a heating scan of a codispersion of DMPE containing 5 mol% α-tocopherol. The profiles were plotted on a logarithmic scale to emphasise the minor bands. Two arrows in Fig. 2 indicate, respectively, the first and second orders of X-ray diffraction patterns of the inverted hexagonal phase. The second-order of the hexagonal-II phase is clearly seen before the first-order lamellar repeat of the liquid-crystal phase first appears.

The presence of 10 mol% α-tocopherol in the phospholipid showed the presence of additional peaks to those of the gel or liquid-crystalline bilayer phases of the pure phospholipid. Fig. 3 shows X-ray diffraction patterns recorded during heating of an aqueous dispersion of 10 mol% α-tocopherol in DMPE. A phase with diffraction spacings indexing to an inverted hexagonal phase appears at 44°C. The scattering intensity and dimensions of the inverted hexagonal phase progressively increase with heating up to the $L_\beta \rightarrow L_\alpha$ transition at 47°C, whereupon its intensity decreases progressively until 50°C. The L_α phase, indexed by two orders of reflection (second-order not shown), appears at 45°C and coexists with the gel and the inverted hexagonal phases up to

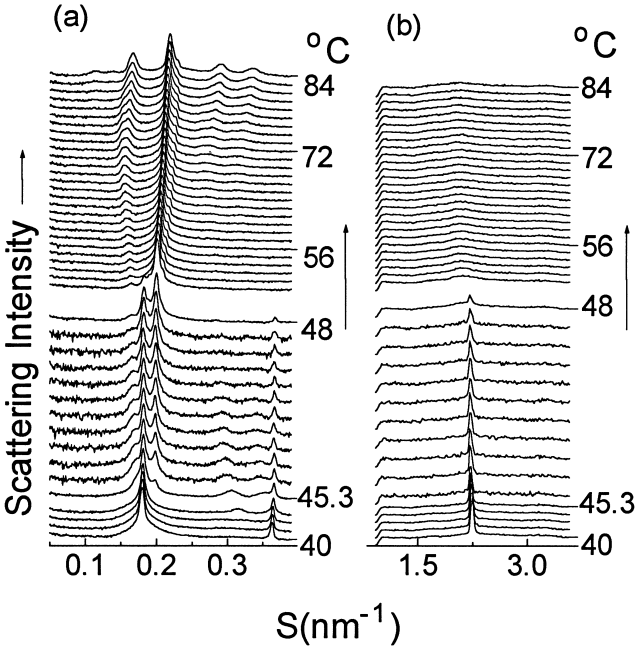

Fig. 3. Plots of successive X-ray scattering intensity profiles in the small-angle region versus reciprocal spacing recorded during heating from 40 to 84°C at 2°/min of a fully hydrated codispersion of 10 mol% α-tocopherol in DMPE in the small-angle (a) and wide-angle scattering region (b). Each diffraction pattern represents scattering accumulated in 20 s (2 s for patterns between 45.3 and 48°C). The profiles in (a) were plotted on a logarithmic scale to emphasise the minor bands.

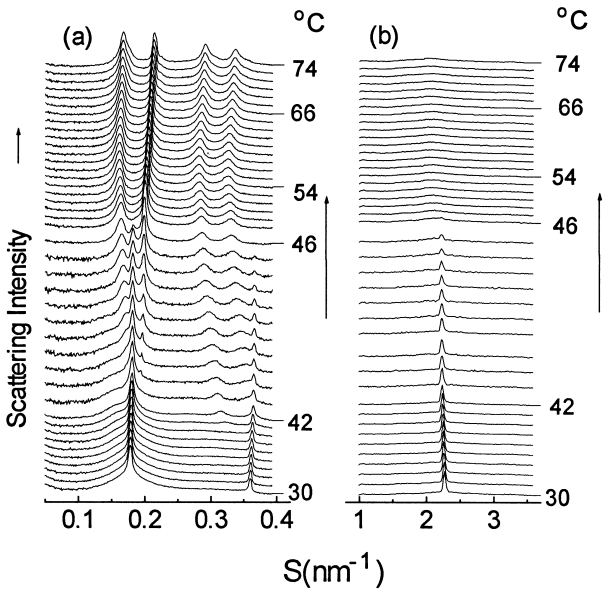

Fig. 4. Plots of successive X-ray scattering intensity profiles versus reciprocal spacing recorded during heating from 30 to 74°C at 2°/min of a fully hydrated codispersion of 20 mol% α-tocopherol in DMPE in the small-angle (a) and wide-angle scattering region (b). Each diffraction pattern represents scattering accumulated in 20 s (5 s for patterns between 42 and 46°C). The profiles in (a) were plotted on a logarithmic scale to emphasise the minor bands.

about 50°C. With further heating, the L_β phase with a lamellar repeat spacing of 5.5 nm disappears from the diffraction patterns and is replaced by an L_α phase with a repeat spacing of 4.9 nm. This coincides with the disappearance in the wide-angle scattering region of the sharp diffraction peak centred at 0.44 nm (at 40°C) and its complete replacement at about 50°C by a broad diffuse diffraction band centred at a spacing of 0.46 nm signifying disordered hydrocarbon chains (Fig. 3b). The intensity of scattering from the inverted hexagonal phase also progressively increases with increasing temperature. Additional diffraction bands are also observed in the scattering patterns. The pattern of change in position of these bands and the emergence of higher-order reflections with increasing temperature allow phase assignments to non-bilayer structures (Fig. 3a). The peak observed at 52°C at a spacing corresponding to 6.2 nm is assigned as a first-order reflection of an inverted hexagonal phase. The peak at 4.7 nm in the pattern recorded at 52°C emerges as the (221) reflection of a Pn3m cubic phase which has a lattice parameter of 12.52 nm at 84°C (see Fig. 7). The absence of a first-order reflection of the cubic phase can be explained by the extinction rule, i.e. due to symmetry within the lattice the structure factors of some indices become zero and no diffraction peak appears.

Increasing the proportion of α-tocopherol in DMPE to 20 mol% eliminated the formation of cubic phases as can be seen from the results presented in Fig. 4. This shows that the H_{II} phase appears around 40°C during a heating scan and coexists with L_β phase (Fig. 4a). The $L_\beta \rightarrow L_\alpha$ phase transition takes place around 44.5°C. Above the phase transition the H_{II} phase coexists with L_α phase and the scattering intensity from the phase increases with increasing temperature. No evidence of any cubic phases was found up to a temperature of 74°C. Only a single symmetrical wide-angle diffraction peak around 0.44 nm is seen which is replaced by a broad diffraction band centred at 0.46 nm with increasing temperature (Fig. 4b).

The effect of α-tocopherol on the gel to liquid-crystalline phase transition of the phospholipid was determined from the X-ray scattering intensity profiles in the wide-angle region. Only single symmetrical reflection peaks were observed in the wide-angle scattering region for all mixtures examined. The normalised scattering intensity of the diffraction peak at 0.43 nm in the gel phase, corresponding to the hexagonal packing of the acyl chains of the phospho-

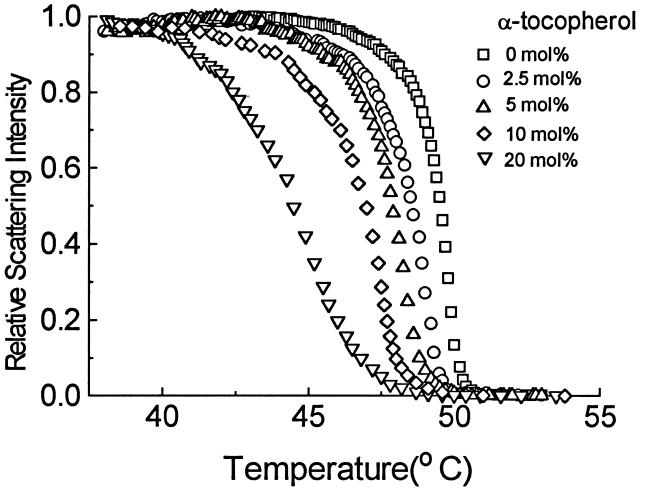

Fig. 5. Normalised X-ray scattering intensities of the wide-angle peaks centred at 0.42 nm recorded from mixed aqueous dispersions of DMPE containing (□) 0; (○) 2.5; (△) 5; (◇) 10; (▽) 20 mol% α-tocopherol.

lipid, are presented in Fig. 5. This shows that with increasing α-tocopherol content, there is a progressive perturbation of the $L_\beta \rightarrow L_\alpha$ phase transition with a broadening of the temperature range over which the transition takes place and a reduction of a few degrees in the temperature of the transition. These data are collated in Table 1 which summarises the structural parameters and transition temperatures obtained from the synchrotron X-ray diffraction analysis of all the mixtures of phospholipid and α-tocopherol examined. The temperature of the $L_\beta \rightarrow L_\alpha$ phase transition (T_m) was determined from the temperature of the mid-point of the change in normalised scattering intensity of the wide-angle gel-phase peak. Consecutive thermal scans indicated that the transitions were essentially reversible with about 2–3°C hysteresis.

Further analysis of the diffraction data obtained from dispersions of DMPE containing 10 mol% α-tocopherol in the gel phase was undertaken to examine the effect of α-tocopherol on the structure of DMPE bilayers. Dispersions equilibrated at temperatures less than 40°C showed diffraction patterns indistinguishable between the pure phospholipid and mixtures containing 10 mol% α-tocopherol (cf. Figs. 1–3). To compare the thickness of the bilayer and water layers in these dispersions, electron density profiles of pure phospholipid and a dispersion of DMPE containing 10 mol% α-tocopherol equilibrated at 20°C were calculated. The profiles were calculated for six orders of reflection, respectively, using the phase combination, +, −, +, −, − established from bilayer swelling methods (Fig. 6a,b). Fig. 6c shows a comparison of the calculated one-dimensional electron density profiles across the lamellar repeat of fully hydrated DMPE in the presence and absence of 10 mol% α-tocopherol. The results show that there is no difference in thickness of the bilayer or water layers which could be accounted by the presence of α-tocopherol in the phospholipid.

Further experiments were performed to characterise the putative cubic phase observed in mixed dispersions of DMPE with 10 mol% α-tocopherol at temperatures above the gel to liquid-crystalline phase transition temperature. Fig. 7 shows a static diffraction pattern of DMPE containing 10 mol% α-tocopherol recorded at 84°C. Six spacings of a cubic phase can be identified with spacings in a ratio of $1/\sqrt{2}$: $1/\sqrt{3}$: $1/\sqrt{4}$: $1/\sqrt{9}$: $1/\sqrt{14}$:$1/\sqrt{17}$. This series is consistent with the index of Pn3m or Pn3 space groups. The $(h^2+k^2+l^2)^{1/2}$ for *hkl* indices vs reciprocal spacings (S^{-1}) fall on a straight line passing through the origin, that supports the cubic phase identification. The reciprocal slope of this line, giving the cubic unit cell lattice parameter, is 12.52 ± 0.01 nm (Fig. 7).

4. Discussion

A number of biophysical techniques have been employed to establish the location of α-tocopherol in model bilayer membranes and its interaction with phospholipids. These studies have led to the conclusion that α-tocopherol significantly perturbs the phase transition between gel and liquid-crystalline phases of saturated phosphatidylcholines [6–10]. Thus, the transition is progressively broadened and the enthalpy decreases with increasing α-tocopherol content until it can no longer be detected.

By contrast, the effect of α-tocopherol on the phase behaviour of phosphatidylethanolamines appears to be considerably more complex with evidence of the formation of separate bilayer phases with different contents of α-tocopherol [9]. When α-toco-

Table 1
Selected d-spacings (*d*), $L_\beta \rightarrow L_\alpha$ transition temperatures (T_m) and the L_β and L_α coexisting temperature range (ΔT_m) in different proportions (*P*) of α-tocopherol in dimyristoylphosphatidylethanolamine

P (mol%)	Lamellar *d* (nm) at 30°C	Chain *d* (nm) at 30°C	Lamellar *d* (nm) at 55°C	T_m (°C) heating	T_m (°C) cooling	ΔT_m (°C) heating
0	5.6	0.42	4.9	49.5	47.6	4.0
2.5	5.6	0.42	4.9	48.6	46.5	4.4
5	5.6	0.42	4.9	48.0	45.8	5.8
10	5.6	0.43	4.9	47.0	44.0	7.0
20	5.6	0.44	4.9	44.5	41.4	8.0

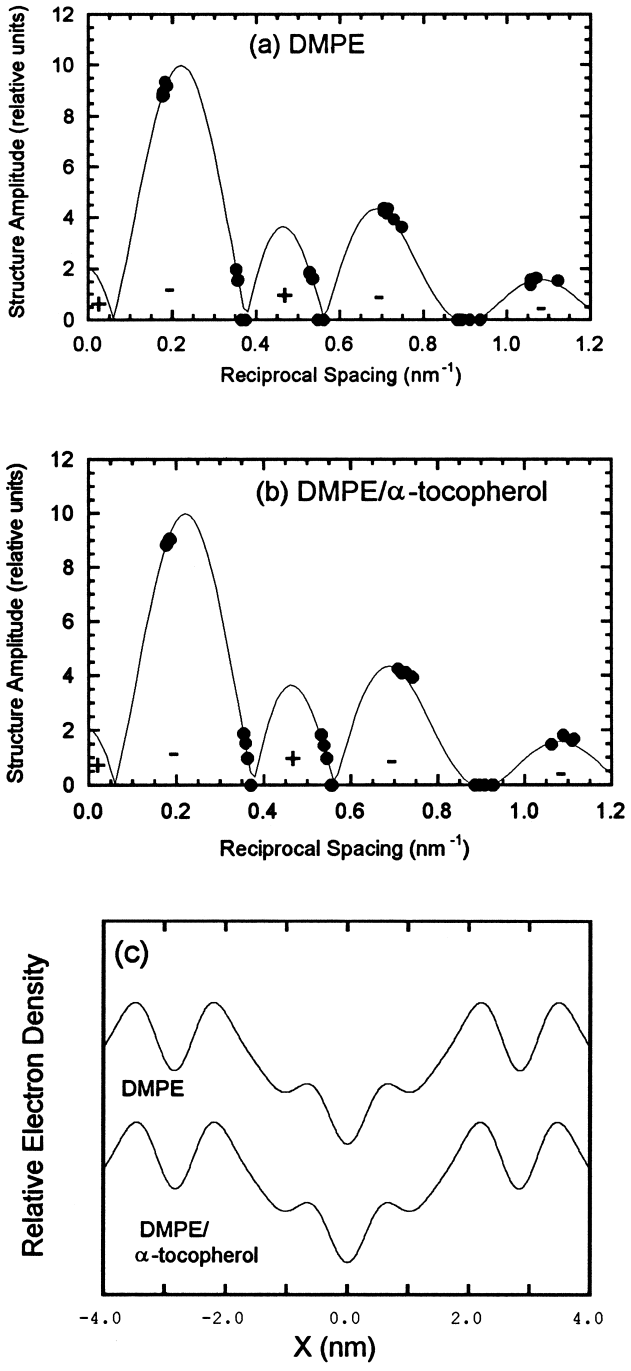

Fig. 6. Structure amplitudes and phase assignments of a dispersion of: (a) pure DMPE; (b) codispersion of DMPE containing 10 mol% α-tocopherol determined at 20°C using osmotic swelling methods; and (c) relative electron density distribution across the lamellar repeat of the two dispersions.

pherol was present in mixtures of phosphatidylcholines and phosphatidylethanolamines the tocopherol molecules are believed to partition into the most fluid phase, irrespective of whether this is composed mainly of the choline or ethanolamine phosphatide [9]. FT-IR studies of DMPE containing α-tocopherol indicated that the phase behaviour was influenced markedly by the hydration state of the phospholipid [15]. The vibration spectra were interpreted to suggest that α-tocopherol produces a rearrangement of the phospholipid molecules, enhancing the hydrogen bonding of the ester C=O groups. Moreover, the results were said to support a model in which α-tocopherol participates directly in hydrogen bonding to the carbonyl oxygen of the acyl ester bonds of the phospholipid via its phenolic OH group, i.e. α-tocopherol intercalates between the phospholipid molecules. No differences could be detected in CH_2 deformation vibrations or PO^{2-} headgroup antisymmetric stretching to indicate that α-tocopherol perturbs the packing of the acyl chains or headgroup motion.

Studies of mixed aqueous dispersions of DMPE and α-tocopherol have already been reported by means of differential scanning calorimetry and ^{31}P-nuclear magnetic resonance technique [14] and the effect of α-tocopherol on the phase behaviour of DMPE is confirmed by the present results. The pure phospholipid undergoes an endothermic transition at about 50°C [14] which corresponds to a disordering of the acyl chains as evidenced by a broad-

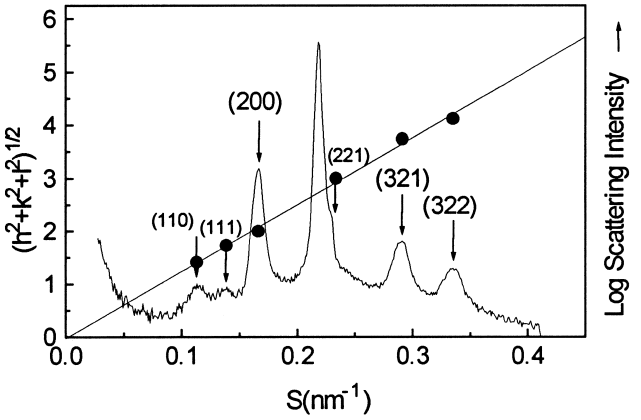

Fig. 7. A static small-angle X-ray diffraction pattern of a codispersion of DMPE containing 10 mol% α-tocopherol recorded at 84°C. Arrows locate expected positions of diffraction peaks of a Pn3m cubic lattice that are indexed (*hkl*). The $(h^2+k^2+l^2)^{1/2}$ for *hkl* indices vs reciprocal spacings (S^{-1}) fall on a straight line. The lattice constant obtained as the reciprocal slope is 12.52 ± 0.01 nm. The biggest peak around 0.22 nm^{-1} is the first order of the liquid-crystalline phase.

ening of the wide-angle scattering peak characterising the gel phase (Fig. 1b). In the presence of increasing amounts of α-tocopherol, the temperature of the main endotherm was found to decrease [14] and this parallels the shift in temperature of the thermal transition observed in the wide-angle scattering profiles (Fig. 5). Additional endotherms at 44°C observed in mixtures containing 10 mol% α-tocopherol in earlier calorimetric studies [14] coincide with the emergence from the lamellar gel phase of an inverted hexagonal phase seen in small-angle scattering profiles during heating. The additional endotherm observed in the earlier calorimetric study at 41°C cannot be explained from the present diffraction data.

There are four possible locations of α-tocopherol in aqueous dispersions of DMPE in the gel phase: (a) in a central hydrophobic domain sandwiched between the two layers of phospholipid; (b) oriented between the phospholipid molecules in bilayer configuration; (c) in a phase-separated domain in the phospholipid; or (d) in the aqueous phase. The wide-angle diffraction band characterising the gel phase is symmetric, indicating that the hydrocarbon chains of the phospholipid are oriented vertically with respect to the bilayer plane. Thus, the presence of α-tocopherol at the centre of the bilayer would be expected to result in a measurable increase in bilayer thickness due to the additional lipid located at the centre of the bilayer. The electron density calculations clearly show that the presence of 10 mol% α-tocopherol in a dispersion of DMPE has no detectable effect on bilayer thickness or width of the intervening water layers. This is not consistent with model a. Model d cannot be excluded from the evidence so far obtained, but is considered improbable on the basis of the lipid solubility of the vitamin.

The remaining models (b and c) cannot be distinguished from each other on the data obtained from the present experiments. Interpolation of α-tocopherol between the phospholipids in bilayer configuration would be expected to cause a decrease in cooperativity of the gel to liquid-crystal phase transition. A decrease in cooperativity of the transition was seen in the present experiments as judged by the temperature range over which half the change in scattering intensity of the wide-angle peak is seen (0.088°/mol% α-tocopherol). This can be compared with the decrease in cooperativity reported for α-tocopherol in dipalmitoylphosphatidylcholine of 0.26°/mol% α-tocopherol. The perturbation is clearly much less in the case of DMPE compared with the choline phospholipid, despite the fact that in the latter, dispersion α-tocopherol forms a stoichiometric complex coexisting with bilayers of pure phospholipid [10]. One explanation could be that domains of DMPE considerably more enriched in α-tocopherol than the 10:1 of phosphatidylcholine/α-tocopherol complex are formed or even domains from which phospholipid is completely excluded coexist with gel phase DMPE bilayers. The presence of such domains in gel phase phospholipid is consistent with the manner of formation of hexagonal-II during heating up through the phase transition of the phospholipid. Thus, phospholipid molecules in the proximity of α-tocopherol domains are induced to form hexagonal-II phase with a low radius of curvature and the repeat spacing of the phase increases as the ratio of phosholipid/α-tocopherol increases. This expansion continues until a stable hexagonal-II structure is formed and the proportion of the phospholipid in hexagonal-II phase compared with bilayer is determined by the stoichiometry of the constituents in hexagonal-II phase. The phase persists at temperatures where the DMPE bilayer is also transformed into liquid-crystal phase indicating that the stoichiometry remains relatively constant. The significance of cubic phase structures and the reason why these occur exclusively in mixtures of DMPE containing about 10 mol% α-tocopherol has yet to be determined.

Acknowledgements

The study was supported by funds provided by the Ministry of Education, Science and Culture, Japan (Monbusho) (H.T. and I.H.), the Daresbury Laboratory, UK and a Cooperative Research Project award from the British Council. X.W. was supported by a K.C. Wong Education Foundation Studentship.

References

[1] M.L. Scott, Fed. Proc. 39 (1980) 2736–2739.
[2] M. Scarpa, A. Rigo, M. Maiorino, F. Ursini, C. Gregolin, Biochim. Biophys. Acta 801 (1984) 215–219.

[3] G.W. Burton, K.H. Ingold, Ann. N.Y. Acad. Sci. 570 (1989) 7–22.
[4] V.E. Kagan, D.A. Stoyanovsky, P.J. Quinn, in: H. Nohl, H. Eserbauer, C. Rice-Evans (Eds.), Inegrated Functions of Coenzyme Q and Vitamin E in Antioxidant Action (Free Radicals in the Environment and Toxiology), Richelieu Press, London, 1994, pp. 221–248.
[5] V.E. Kagan, Ann. New York Acad. Sci. 570 (1989) 121–125.
[6] J.B. Massey, H.S. She, H.J. Pownall, Biochem. Biophys. Res. Commun. 106 (1982) 842–847.
[7] E.J. McMurchie, G.H. McIntosh, J. Nutr. Sci. Vitaminol. 32 (1986) 551–558.
[8] J. Villalain, F.C. Aranda, J.C. Gomez-Fernandez, Eur. J. Biochem. 158 (1986) 141–147.
[9] A. Ortiz, F.C. Aranda, J.C. Gomez-Fernandez, Biochim. Biophys. Acta 898 (1987) 214–222.
[10] P.J. Quinn, Eur. J. Biochem. 233 (1995) 916–925.
[11] K. Ohki, T. Takamura, Y. Nozawa, J. Nutr. Sci. Vitaminol. 30 (1984) 221–234.
[12] T. Ohyashiki, H. Ushiro, T. Mohri, Biochim. Biophys. Acta 858 (1986) 294–300.
[13] R.H. Bisby, D.J.S. Birch, Biochem. Biophys. Res. Commun. 158 (1989) 386–391.
[14] V. Micol, F.J. Aranda, J. Villalain, J.C. Gomez-Fernandez, Biochim. Biophys. Acta 1022 (1990) 194–202.
[15] J. Salgado, J. Villalain, J.C. Gomez-Fernandez, Biochim. Biophys. Acta 1239 (1995) 213–225.
[16] A. Blume, R.G. Griffin, Biochemistry 21 (1982) 6230–6242.
[17] R.M. Epand, R. Bottega, Biochemistry 26 (1987) 1820–1825.
[18] J.J. Cheethan, E. Wachtel, D. Bach, R.M. Epand, Biochemistry 28 (1989) 8928–8931.
[19] H. Takahashi, K. Sinoda, I. Hatta, Biochim. Biophys. Acta 1289 (1996) 209–216.
[20] B.A. Cunningham, W. Bras, P.J. Quinn, L.J. Lis, J. Biochem. Biophys. Methods 29 (1994) 87–111.
[21] C. Boulin, R. Kempf, M.H.J. Koch, S.M. McLauchlin, Nucl. Instr. Methods Phys. Res. A249 (1986) 399–407.
[22] A. Bigi, N. Roveri, in: S. Ebashi, M. Koch, E. Rubenstein (Eds.), Fibre Diffraction: Collagen (Handbook on Synchrotron Research, Vol. 4), Elsevier Science, Amsterdam, 1991, pp. 25–37.
[23] E.J. Addink, J. Beintema, Polymer 2 (1961) 185–193.
[24] C.R. Worthington, A.E. Blaurock, Biophys. J. 9 (1969) 970–990.
[25] D. Sayre, Acta Crystallogr. B. 5 (1952) 843–848.
[26] J. Torbet, M.H.F. Wilkins, J. Theor. Biol. 62 (1976) 447–458.
[27] N.P. Franks, J. Mil. Biol. 100 (1976) 345–358.
[28] G.I. King, C.R. Worthington, Phys. Lett. 35A (1971) 259–260.
[29] T.J. McIntosh, S.A. Simon, Biochemistry 25 (1986) 4058–4066.